



Contents lists available at ScienceDirect

International Journal of Rock Mechanics and Mining Sciences

journal homepage: www.elsevier.com/locate/ijrmms

Full-scale experimental investigation of the performance of a jet-assisted rotary drilling system in crystalline rock

Thomas Stoxreiter^{a,*}, Gary Portwood^b, Laurent Gerbaud^c, Olivier Seibel^d, Stefan Essl^e,
Johann Plank^f, Herbert Hofstätter^g

^a Montanuniversität Leoben, Chair of Subsurface Engineering, Erzherzog Johann Straße 3, 8700 Leoben, Austria

^b Smith Bits, A Schlumberger Company – Smith International Italia S.p.A, Via Traversa 50, 56048 Saline di Volterra, Italy

^c MINES ParisTech, PSL University, Centre de géosciences, 35 rue St Honoré, 77300 Fontainebleau, France

^d ES-Géothermie, Boulevard du Président Wilson 26, 67932 Strasbourg, France

^e RAG Energy Drilling GmbH, Schwarzmoos 28, 4851 Gampern, Austria

^f Technische Universität München, Chair of Construction Chemistry, Lichtenbergstraße 4, 85747 Garching, Germany

^g Montanuniversität Leoben, Chair of Petroleum and Geothermal Energy Recovery, Parkstraße 27, 8700 Leoben, Austria



ARTICLE INFO

Keywords:

Drilling technology
Geothermal energy
Rock mechanics
ThermoDrill

ABSTRACT

Full-scale drilling experiments (8½ in. bit size) with a high-pressure fluid jet assisted rotary drilling system were performed in hard to drill crystalline rock. Besides the development of novel drill bits and high-pressure components, an existing drilling simulator test bench was adapted to the requirements of the current tests. A total number of seventeen test runs was conducted to enable a comparison of drilling performance between state of the art drilling technique and the innovative jet assisted system. A significant increase in rate of penetration was achieved with the system. Another relevant aspect was the influence of different drilling and jetting fluids on drilling performance. The interaction of the hydraulic and mechanical rock removing processes was researched in detail and led to further conclusions about the rock destruction process. Basic and sophisticated correlations between drilling parameters were examined in order to define the favourable operational parameters for each bit type. Lessons learned during these experiments will directly be integrated in the preparation of later field tests of the enhanced system.

1. Introduction

The utilisation of enhanced geothermal systems (EGS) is one of the future cornerstones of Europe's renewable energy strategy. Because of the great depth of suitable geothermal reservoirs, drilling costs often represent more than half of the total costs of EGS, as well as an important share in CO_{2eq} emissions regarding their Life Cycle Analysis. One possible option to reduce the drilling costs is to increase the rate of penetration (ROP). Therefore an advanced drilling technology is currently under development within the framework of the EU research project “ThermoDrill”, where the core element of the project is a hybrid drilling system consisting of conventional rotary drilling in combination with high pressure fluid jetting.

A detailed investigation on the jet cutting performance in various ambient pressure regimes is given in 1. The results are in accordance with the findings of 2, 3 and 4. The stand-off distance as well as the hydraulic power of the high pressure jet, defined by pressure and flow

rate, and the back pressure were identified as the key parameters for an adequate jet cutting performance. Based on these data, specifications for the hydraulic part of the drilling system were set. In order to validate the given data and to gain more detailed information about the system performance under realistic drilling conditions, full-scale laboratory experiments were performed.

Both full-scale and scaled-down drilling experiments have been performed extensively in the last sixty years, pursuing different ambitions. Usually the goal was to increase the ROP in oil and gas related formations by identifying the restricting mechanism and defining procedures to eliminate this mechanism. Early investigations^{5,6} revealed the basic relationships between weight on bit (WOB), rotary speed and the ROP for several bit types and proposed optimum operating parameters. Other researchers^{7,8} soon noticed the great influence of differential pressure on ROP. Related to that conclusion, a great part of the subsequent research was focused on improving bottom hole cleaning efficiency. Effects such as static and dynamic chip hold down, balling-

* Corresponding author.

E-mail address: thomas.stoxreiter@unileoben.ac.at (T. Stoxreiter).

<https://doi.org/10.1016/j.ijrmms.2019.01.011>

Received 26 July 2018; Received in revised form 20 November 2018; Accepted 28 January 2019

Available online 06 February 2019

1365-1609/© 2019 The Authors. Published by Elsevier Ltd. This is an open access article under the CC BY license (<http://creativecommons.org/licenses/by/4.0/>).

up of the hole bottom and the drill bit, the effects of pore pressure and mud filtration and many other factors were investigated in great detail for permeable and impermeable formations. Further, the influence of the overburden pressure, mud pressure and formation pressure on the drilling performance was a topic of great interest and intense research e.g. 9–13. Also the effect of tool parameters such as bit size¹⁴ and bit hydraulics^{15,16} was evaluated. Early approaches^{17,18} were undertaken to relate the ROP to other drilling parameters and thus be able to predict the ROP for unknown conditions. A comprehensive experimental study with various types of full-scale drill bits under simulated deep drilling conditions with the goal to increase the ROP was performed,¹⁹ and delivered relevant information on major influencing factors, including a detailed drilling fluid analysis.

Full-scale and scaled-down experiments were not the only means used to investigate the drilling process. A vast number of indentation, scraping, and indexing tests enabled gathering valuable information about the rock destruction by single inserts or cutters. Specially related to the current task, laboratory tests were performed^{20,21} with PDC and disc cutter elements on pre-jetted rock samples. These tests showed the favourable impact of jet kerfs on the mechanical rock removing process. In the context of the current paper the term "kerf" is mainly related to the rock volume removed by the high-pressure fluid jets, regardless of the geometric dimensions of the removed volume. Detailed studies about dynamic confinement²² and dynamic pore pressure ahead of the bit²³ explored the influence of the drilling process on the behaviour of the affected rock mass and vice versa. However, the extent of existing information is immense, and many aspects of the drilling process and related mechanisms are well known. Using this knowledge enables the restriction of the experimental campaign to only specific project-related tasks.

Despite the huge number of publications on these drilling processes, there exists only few literature about laboratory experiments on high pressure jet assisted drilling, especially in full-scale. Particular information is provided about the influence of jets on the bottom hole cleaning efficiency in 24,25 but this topic is only partly related to the current paper. Certainly, in the 1990s a comprehensive laboratory and field testing research study on a variety of sedimentary rocks, marble and subordinate on granite, using high pressure jet assisted roller cone bits was performed. The related results, reported in 26 and 27 demonstrate the great potential of this technology. Further, the outputs are used as a guideline and for comparison to the current experiments.

Beside these two publications, both were related to the same research framework, the authors are not aware of any other published research concerning full-scale or even scaled-down laboratory experiments on high pressure jet assisted rotary drilling. As the future application of the "ThermoDrill" system lies in geothermal applications, often in crystalline rock, the current experiments were conducted in hard to drill granite. In the context of this paper, the term hard to drill means low ROP values during drilling. Hence, the present paper is the first comprehensive study of high pressure jet assisted rotary drilling in crystalline rock. Further, all reported previous experiments were conducted with standard three-cone bits with only one high pressure nozzle tower respectively one extended nozzle. The present study was performed with three bits from the same manufacturer, with the same cutting structure, but integrating newly developed high pressure bodies and up to two high pressure extended nozzles. Novel aspects about the mechanism of combined hydraulic and mechanical rock excavation are provided. Another enhancement is the comparison of tap water and two common mud types both as a high pressure jetting medium and standard drilling fluid. Thanks to the measured and monitored drilling conditions in combination with the almost perfectly homogenous rock samples, with in detail determined mechanical and physical properties, full-scale experiments provided the ideal environment to validate the presented concept and to identify potential improvements for later field tests.

As a final stage, the new high pressure jet assisted drilling system



Fig. 1. Full scale drilling test bench.

will be tested in the field, keeping in mind that the spectrum of unknown or only estimated influencing variables is much greater than in the laboratory tests. Given the associated financial expenditures and risks associated with field tests, it is a little surprising that more literature exists about field tests of high pressure jet assisted drilling than full-scale lab tests. As a consequence of the promising results of the large-scale laboratory experiments, several test runs in the field were successfully performed.^{27,28} In addition, other researchers, who supplied the high pressure from surface,²⁹ or using two innovative types of downhole intensifiers,³⁰ conducted field tests with high pressure jet assisted drill bits. Although the technical implementation was different for each study, the majority of the reported results revealed a significant increase in ROP because of the high-pressure fluid jets.

2. Experimental setup

2.1. Drilling simulator test bench

The tests were conducted at the drilling simulator test bench of Mines ParisTech, located in Pau, France (Fig. 1). The test bench allows full-scale drill bit tests by simulating deep drilling conditions (up to 5000 m) and direct comparison between different bits or drilling technologies as all aspects are controllable and reproducible. The common testing procedure consists of drilling a rock sample exposed to a pressure similar to the borehole pressure. The rock sample is held in a pressure vessel (Fig. 2) with constant overburden pressure, confining pressure and pore pressure. WOB (up to 245 kN) can be applied with two lateral pistons and the rotation of the bit (up to 1000 RPM) is generated with a DC electric motor placed on the bench platform. The motor is connected to the drill shaft through a gear box. The drilling fluid is injected at the bit through the drill pipe with a PL7 Gardner Denver pump and the pressure is controlled with the opening of a valve. Table 1 provides the overall drilling test bench capabilities.

Tests were done with WOB control, so the pressure in the pistons

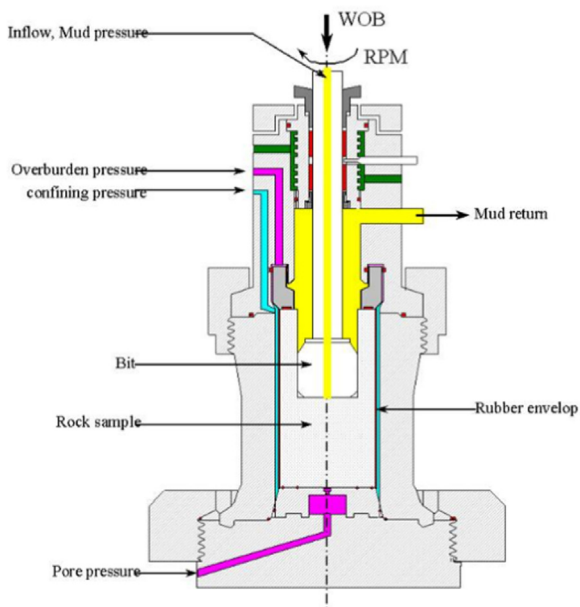


Fig. 2. Pressure vessel of the drilling test bench.

Table 1

Overall drilling test bench capabilities.

Parameter	Maximum capabilities
WOB, kN	245
RPM, rev/min	1000
Torque, dNm	500
Overburden pressure, MPa	70
Confining, down hole and pore pressure, MPa	50
Drilling length, mm	480

was continuously adjusted to follow the WOB control input. During the testing, physical parameters were measured with transducers. The different types of pressure (overburden, injection, down hole, confining and pore) and temperatures were continuously recorded. WOB and torque were measured close to the bit with strain gages fixed on the drill shaft while the rate of penetration was measured by differentiating the bit position, obtained with a magneto-restrictive transducer, by time. The whole set of data was recorded at a high sampling rate of 200 Hz. Subsequently the data was stored in ASCII files.

2.2. Modifications to the test bench for high pressure supply

The original test bench was not designed for high-pressure jet-assisted drilling experiments. Therefore, several modifications and supplements were necessary to integrate the high-pressure tubing, illustrated in Fig. 3. The modifications included the installation of a tee and knee to provide two inflow ports. At the top of the tee, a special designed cap was mounted which was both, pivot point and sealed conduit for the HP-tube. Above the cap, a high pressure swivel provided the rotation free connection of the high pressure hose coming from the pump truck and the pressure transducer to the HP-tubing. Inside the drill collar, the HP-tubes connecting the drill bit to the swivel were made up with sleeves. The high pressure was supplied by a mobile URACA Jet Power 300–1000 pump with a maximum flow rate of 55 L/min at 250 MPa. The pressure losses along the HP-tubing below the pressure transducer were determined with preliminary tests and were in the range of 5–10 MPa for an initial pressure of 240 MPa. Because of a great interest in the alteration of rheological properties of the jetted medium due to pressurization, hoses were mounted to take fluid samples before the medium exists the nozzle. This was possible because the

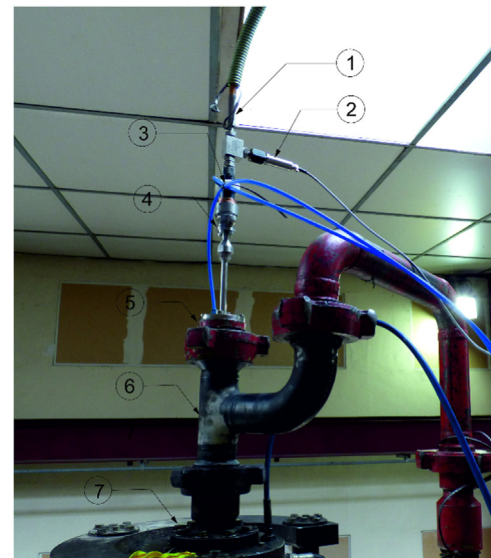


Fig. 3. Modified top part of the drilling simulator: 1) high pressure hose, 2) HBM P3MB pressure transducer, 3) hoses for fluid sampling, 4) high-pressure swivel 5) HP-tube conduit/bearing 6) tee with knee 7) ordinary wash pipe.

high pressure swivel was equipped with a gap seal which had desired leakage. All parts were either connected with sleeves or collar and gland.

2.3. Drill bits, rock properties and drilling fluids

The tested bits included a standard bit (Fig. 4c) to establish a baseline and proof the method of measurement as well as two novel roller cone drill bit designs, see Fig. 4a and b. The two patent pending drill bits (IADC 627Y) were designed and manufactured by Smith Bits. The design breaks away from traditional standard roller cone designs and incorporates novel concepts adapted to fit the high pressure requirements. To ensure optimal comparability, all three bits had the same cutting structure, the three cones and the cutting elements were exactly the same on all three bits. As base model, a hard formation TCI (Tungsten Carbide Insert) bit (IADC 627Y) was used, that is typically deployed in deep granite drilling applications. The pin connection was a 4–1/2 in. standard API connection.

Instead of using and modifying an existing standard roller cone bit, as done in previous projects, the innovative bit designs had a separate high pressure body with a conduit/plenum system that was independent of the bit body's internal low-pressure hydraulic conduit/plenum, but still an integral part of the bit body. That enabled a separate low-pressure fluid communication through at least one low-pressure nozzle with sufficiently high flow rate to ensure proper hole cleaning and cuttings removal. In the frame of this paper, the conventional fluid flow through the bit with the purpose of cooling and cleaning the bit, carrying out the cuttings etc. was termed as low-pressure flow through common nozzles. In contrast, the additionally implemented high pressure system with a pressure up to 220 MPa was jetting the fluid through extended high pressure nozzles and had the purpose to create kerfs in the borehole bottom and thereby increase the ROP. This means that the one-nozzle bit had two low-pressure nozzles and one high-pressure nozzle and the two-nozzle bit had two high pressure nozzles and one low-pressure nozzle. The specifications of all three bits are summarized in Table 3.

The high pressure nozzles were made out of hardened steel without any inserts, supplied by URACA GmbH & Co. KG with a nozzle discharge factor of 0.97. The two-nozzle bit was equipped with either 0.9 mm diameter or 1.1 mm diameter nozzles, depending on the pressure. A different radial position, in terms of radial distance from the bit



Fig. 4. Novel drill bits: a) one-nozzle bit and b) two-nozzle bit and c) the baseline bit.

Table 2

Mechanical and physical properties of Neuhauser granite.

Density, g/cm ³	2.7
Porosity, %	3.0 ³²
Permeability, mD	0.07–0.00 ³²
Young's modulus, GPa	67.0 ± 7.8
UCS, MPa	145.0 ± 31.3
UTS, MPa	10.0 ± 1.4
Jetting threshold pressure, MPa	100.0 ¹

axis, of 3–4 mm between the two extended nozzles increased the affected area. The one-nozzle bit had one nozzle with either 1.3 mm diameter or 1.5 mm diameter. The nozzle holders were available at different lengths in order to change the stand-off distance (distance between nozzle outlet and rock surface) as required. The standard stand-off distance was 6–8 mm, relative to the radial position, and it could be changed to 10–12 mm.

The tested rock type was Neuhauser granite, a fine- to medium grained granite from the Bohemian Massif. Predominant mineral phases are quartz, feldspar and biotite. The samples were extracted from a quarry in Upper Austria. The dimensions of the samples fit the requirements by the test bench with a diameter of 310 mm and a height of 380 mm. The mechanical and physical rock properties are listed in Table 2. Regarding the permeability, Neuhauser granite was characterized as impermeable although the permeability varied between 0.07 mD and a value, too small to be measured by the device (equals 0.0 mD).

The two tested water based mud types were provided by the Chair of Construction Chemistry at the Technical University Munich and Sirius-ES Handels GmbH. One mud system was specially designed for geothermal applications by the Chair of Construction Chemistry and was based on sepiolite and KCL, while the properties of the other mud type were mainly determined by the bio-polymer xanthan gum and KCL. The exact formulations are not given due to nondisclosure agreements. The density for both fluids was around 1.1 g/cm³. The third drilling/jetting medium was tap water. Subsequently the different mud types will be only labelled as water; sepiolite and xanthan gum.

2.4. Testing procedure

The testing procedure was partly based on the work described by 26 and 27 since the test bench capabilities were similar. Due to the broad knowledge about the influencing parameters on the drilling process, many aspects were not particularly considered in the test plan and the experiments were focused on the investigation of the impact of the high pressure fluid jets. According to earlier conclusions^{9–13} the overburden and confining stress do not significantly affect the ROP. Therefore, the confining stress was set equal to mud pressure and the overburden stress was set to a value which prevented the rock sample from rotating with the drill bit (up to 30 MPa). The differential pressure between the mud pressure and the formation pore pressure was identified as one major impact factor.⁸ Neuhauser granite has a low porosity and is quasi impermeable, especially during the short duration of testing and since all rock samples were mounted in a dry state, the formation pore pressure was negligible. As the effective-stress law is valid for impermeable rocks, according to 9, the effective stress state in the rock was hydrostatic, except in the region influenced by the rock destruction process. The samples were sealed off at the bottom and the top. The differences in measured pressure of the mud after exiting the bit in the drilled hole (mud pressure) and the measured confining pressure were negligible, see Fig. 5. The mud supply had an actual average injection pressure of 11 MPa at a flow rate of 600 L/min, measured 8 m before the bit in the conventional mud supply line. Consequently, a pressure drop of around 1.0–1.4 MPa across the drill bit occurred, resulting in a mud pressure of around 10 MPa. The mud pressure was controlled by a

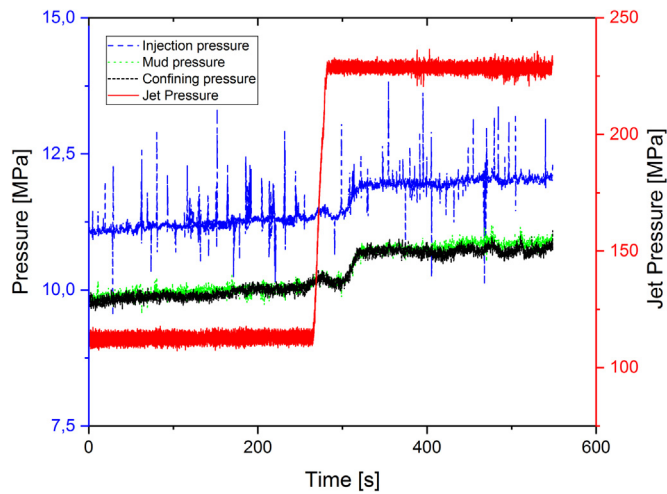


Fig. 5. Fluid pressures measured during experiment with one-nozzle bit with 220 MPa.

valve in the return line and was actually limited to 10 MPa. Fig. 5 shows exemplarily the relationship between the various pressure measurements during a one-nozzle bit testing with 220 MPa jet pressure and water as drilling fluid. After engaging the drill bit about 4 cm (around 240 s) into the rock sample, the jet pressure was changed from approx. 110 MPa to the desired value of approx. 220 MPa at the bit. Accordingly, injection pressure, mud pressure and confining pressure were increased simultaneously by approx. 1 MPa, probably because the valves were not capable of regulating the additional flow perfectly. The measured pressure drop across the bit Δp could also be estimated by applying the well-known equation:

$$\Delta p = \frac{\rho Q^2}{2c_d^2(TNFA)^2} \tag{1}$$

but for SI units, given by,³¹ using the suggested nozzle coefficient c_d of 1.03. The parameters with the correct units and the associated results are shown in Table 3, where the measured and the calculated values are in good correlation. Obviously, these calculations do not include the high-pressure flow, since it was not contributing to the pressure drop across the drill bit. Hence, the flow rate Q was 600 L/min, the Total Nozzle Flow Area (TNFA) was depending on the bit type and number of low-pressure nozzles just as the fluid density ρ on the type of fluid used.

The rotational speed was set constant at 60 RPM for all tests and the weight on bit varied between 45 kN and 150 kN. The WOB was measured via strain gauges, applied at the drill shaft close to the drill bit, and the pressure in both pistons. The measurement system was calibrated to provide the reading in metric tons, which were subsequently converted to kN with a conversion factor of 9.8. In total, seventeen tests were performed with altered parameters as summarized in Table 4. The stand-off distance for the extended nozzles was set constant at the closest possible value, around 6–8 mm, for all experiments.

The procedure remained the same for all tests, except the obvious operational differences between tests with and without jet-assisted drill

Table 3
Parameters to calculate the pressure drop across the drill bit.

Bit type	Standard bit			one-nozzle bit		two-nozzle bit
Number of nozzles	3	3	3	2	2	1
Nozzle diameter, mm	9.525	9.525	9.525	11.113	11.113	15.875
Total Nozzle Flow Area (TNFA), mm ²	213.76	213.76	213.76	193.99	193.99	197.93
Flow rate, m ³ /s	0.01	0.01	0.01	0.01	0.01	0.01
Fluid type	Water	Sepiolite	Xanthan gum	Water	Sepiolite	Water
Fluid density, kg/m ³	1000	1100	1100	1000	1100	1000
Pressure drop across the drill bit, MPa	1.03	1.13	1.13	1.25	1.37	1.20

Table 4

Testing parameters of all performed tests. *Rock sample broke during the experiment.

Test	Bit type	Drilling fluid	Pressure at the bit	HP nozzle flow rate	HP nozzle diameter	HP hydraulic power	
			MPa	L/min	mm	kW	
1	Standard	Water	-	-	-	-	
2			-	-	-	-	
3			-	-	-	-	
4			-	-	-	-	
5	Sepiolite	-	-	-	-	-	
6			-	-	-	-	
7			-	-	-	-	
8	Xanthan gum	-	-	-	-	-	
9			-	-	-	-	
10	one-nozzle	Water	115	50.9	1.5	97.6	
11			220	54.1	1.3	198.4	
12		Sepiolite	-	-	-	-	
13			-	-	-	-	
14			-	-	-	-	
15		two-nozzle	Water	115	54.8	1.1	105.0
16				220	51.9	0.9	190.3
17	-			-	-	-	

bits. After the rock sample was mounted and the cell was lowered, the overburden and confining pressure were established, followed by the mud pressure and mud flow. Subsequently, the bit was slowly engaged in the rock to a distance of around 4 cm to ensure consistent conditions. During this step, the high pressure was already applied at the lowest pressure possible, between 110 MPa and 140 MPa to avoid particles entering the HP line. Afterwards, the WOB was raised to defined levels between 45 kN and 150 kN, usually in 49 kN steps. The WOB was held constant until a quasi-static state was reached, typically developing within roughly ten seconds, and a sufficient number of data points was sampled at the quasi-static state. After reaching the final depth, the drill collar was raised while the low-pressure fluid circulation and the high pressure supply were shut down simultaneously.

3. Results and discussion

3.1. Comparison of drilling performance with water

The goal of the experiments was to quantify the impact of jet-assisted drilling on the ROP compared to conventional rotary drilling. Fig. 6 shows the results of drilling simulator tests with tap water as drilling and jetting fluid. A linear regression analysis was performed and the lines of best fit are included in Fig. 6. With a minimum coefficient of determination of 0.99, the assumed linear relationship between the ROP and the WOB was approved. For reasons of clarity, the printed data points represent the mean values of all experiments with the same bit type at similar WOB. The lines of best fit were equal and the coefficient of determination was still at least 0.99 if all data points were used for the regression analysis, so no results were distorted because of this procedure. The regression analysis was based on the

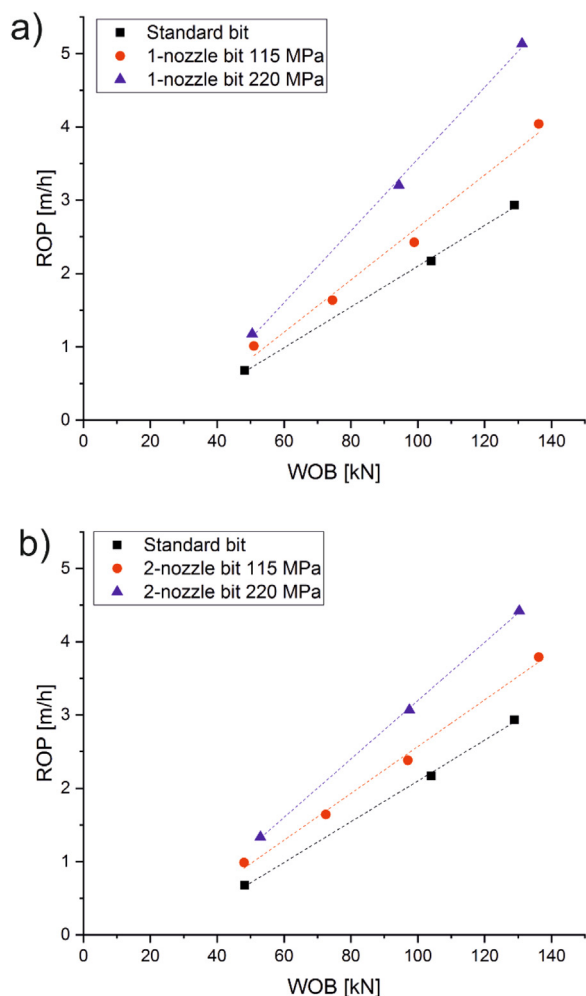


Fig. 6. Drilling performance with water.

Table 5 Summarized results of the regression analysis.

Bit type	Fluid	Jet pressure (MPa)	A (m/h/kN)	B (m/h)
Standard	Water	–	0.0278	0.6787
two-nozzle	Water	115	0.0319	0.6203
	Water	220	0.0398	0.7834
one-nozzle	Water	151	0.0357	0.9421
	Water	220	0.0490	1.3345
Standard	Sepiolite	–	0.0278	0.6789
Standard	Xanthan gum	–	0.0264	0.7442

following simple equation, with the coefficients summarized in Table 5:

$$ROP = A \times WOB - B \tag{2}$$

Obviously, the ROP depends directly on the WOB, as expected for roller cone bits. Although the correlation was linear, the “ROP increase” was not a constant value. The term “ROP increase” means the proportional enhancement of the ROP compared to the ROP of the standard bit. For a clearer description of the results, the “ROP increase” is plotted against the total hydraulic power at the drill bit in Fig. 7. Any particular ROP-value was calculated from the regression analysis in order to get the values exactly for 49, 98 and 147 kN weight on bit instead of the incomparable measured values. This procedure seems appropriate regarding the excellent coefficient of determination. The hydraulic power of the conventional nozzles was calculated with 10.0 kW, assuming a pressure drop across the bit of 1 MPa at 600 L/min. The maximum measured and also the maximum analytical estimated pressure drop of

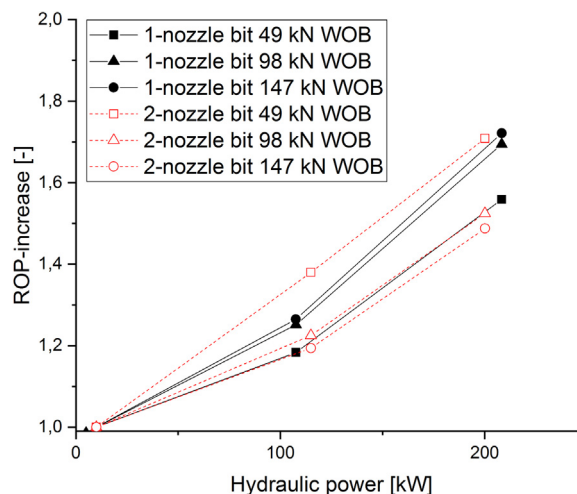


Fig. 7. ROP increase versus total hydraulic power at the bit.

ca. 1.4 MPa would result in a hydraulic power of 14 kW. For reasons of clarity and simplicity in the later explanations, the hydraulic power of the conventional nozzles was set constant to 10 kW, where the possible difference of 4 kW results in a maximum error of less than 4%. The HP nozzle hydraulic power is illustrated in Table 4; the sum of both was defined as the total hydraulic power at the bit. The results indicated a constant increase of ROP with increasing hydraulic power at the bit respectively the high-pressure jets. This trend was obviously only valid for the range of hydraulic power and weight on bit tested. The change of the gradient was not distinct but still noticeable for most of the curves and was probably attributed to the nearly doubled jet pressure from approx. 100 kW to around 200 kW hydraulic power, which most likely improved the cutting performance of the high pressure jet.

A very interesting effect was observed when the “relative ROP increase” was calculated and compared to the weight on bit, see Fig. 8. The “relative ROP increase” is defined as ROP increase at 98 kN and 147 kN weight on bit compared with the ROP increase at 49 kN WOB. Nearly the same behaviour was observed for tests with lower and higher values of hydraulic power, but completely contrary results were noticed for the one-nozzle bit and the two-nozzle bit. While the one-nozzle bit improved its performance with increasing WOB, with an increasing rate, the two-nozzle bit showed a performance increase with decreasing rate with increasing WOB. In other words, the two-nozzle bit exhibited the best drilling performance at low weight on bit. It took approx. 59 kN with 220 MPa jet pressure and 84 kN with 115 MPa jet

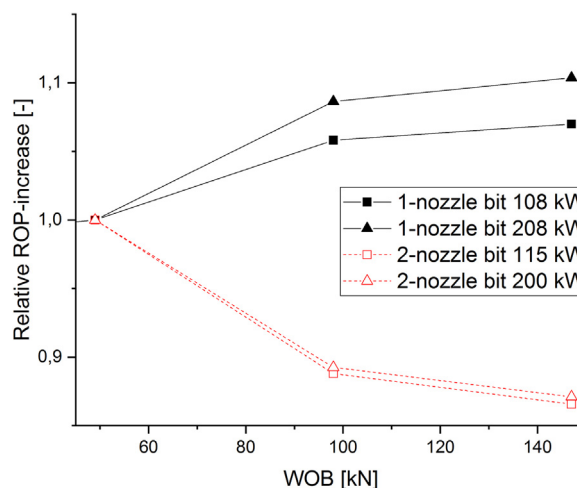


Fig. 8. Relative ROP increase versus weight on bit.

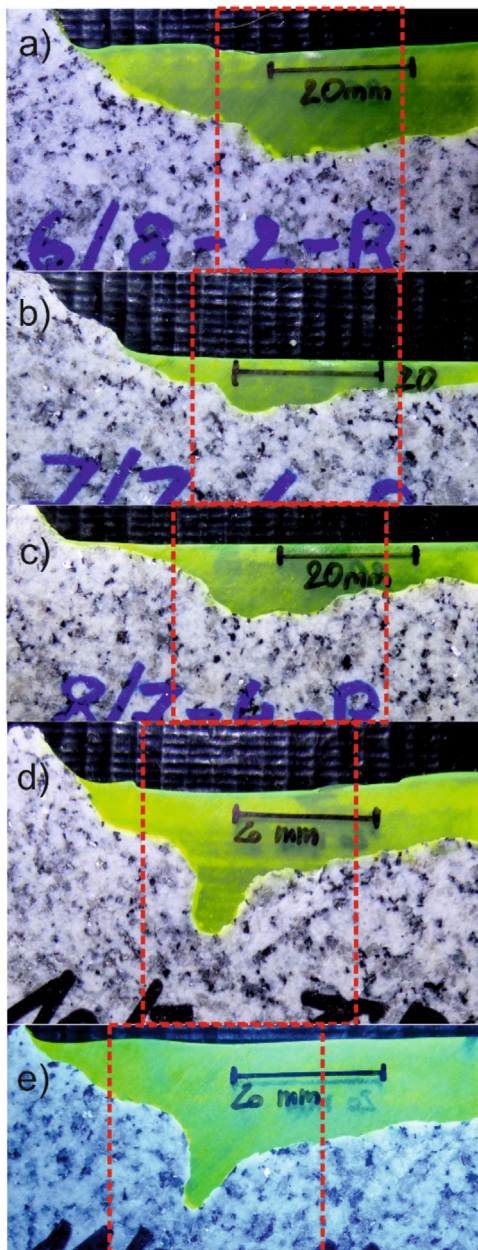


Fig. 9. Cross section of the borehole bottom: a) two-nozzle bit at 220 MPa b) two-nozzle bit at 115 MPa c) one-nozzle bit at 115 MPa d) one-nozzle bit at 220 MPa e) one-nozzle bit at 220 MPa sepiolite based fluid.

pressure until the one-nozzle bit outperformed the two-nozzle bit. These observations were a direct measure of the efficiency development of the technology with regards to WOB. The two-nozzle bit was more efficient at low WOB than the one-nozzle bit and vice versa. This circumstance is also represented by the coefficients A and B in Table 5 and is a very important outcome for later applications.

Fig. 9 shows cross sections of the hole bottom for different experiments, where the area of the jet cut is marked by the dotted lines. The samples were extracted via core drills from the borehole bottom and subsequently saturated with fluorescing epoxy resin for later investigations. However, the results were not completely representative due to the possibility that the high pressure jet was cutting the same trace several times. But it is a good basis for qualitative considerations and the estimated cutting depth assorted well with the findings by 1 for the same type of rock. Obviously, the one-nozzle bit created by far the deepest and well-formed kerf with 220 MPa jet pressure, while a jet

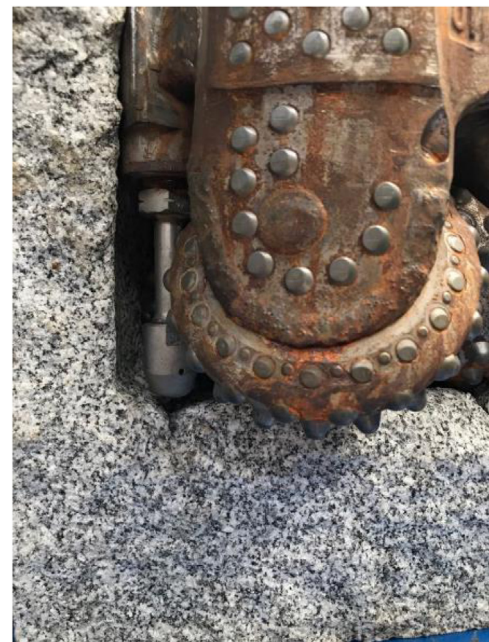


Fig. 10. One-nozzle bit integrated in a drilled rock sample.

pressure of 115 MPa generated wider kerfs, which was eventually attributed to the decay of the jet at the applied standoff distance. The two-nozzle bit generated wide jet kerfs throughout, where only the depth appeared to be a little larger for the 220 MPa jet pressure. Fig. 10 illustrates the position of the extended nozzle and the deep created jet kerf with the one-nozzle bit.

One reason for these results could be related to the findings of 27 and 33. Apparently, there exists an optimum distance between a free surface (kerf or crater) and the indentation depth of the inserts, as well as an optimum kerf depth related to the insert penetration depth. Beyond this optimum distance and depth, the rock removing process is less efficient. Due to the wider affected area in combination with the relatively small penetration depth of the inserts at low WOB, the two-nozzle bit eventually reached more optimal conditions. By contrast, the one-nozzle bit created deeper cuts, but in a narrower area. When the WOB increased, the penetration depth of the inserts increased, and the effect of a deeper cut became more and more important and improved the efficiency of the one-nozzle bit drilling process. The subsequent consideration of the specific energy supports that theory. Furthermore, at low weight on bit, the penetration of the inserts in the rock surface was very shallow. Even the relatively shallow kerf, created by the two-nozzle bit or the one-nozzle bit at lower jetting pressure, might have been deep enough that particular inserts did not penetrate the hole bottom at all. Associated, these inserts had no contact and the force redistribution led to a higher rate of penetration. This effect would have been more pronounced for the two-nozzle bit due to the wider affected area. Both bit types had in common that the high-pressure nozzles were located at a radial position where the mechanical rock removing was most difficult. By creating kerfs in that area, the whole drilling process was positively affected.

Another possible effect that might have attributed to the ROP enhancement was the “bottom hole cleaning”. In this paper the term “bottom hole cleaning” defines the process of removing rock chips from the borehole bottom against hold down forces, whereby this definition applies for the localized area affected by the impinging jet as well as for the whole borehole bottom. From Fig. 9, it is clear that even at lower jetting pressures, kerfs were created by the jets. Certainly, the created kerfs must not necessarily be the only beneficial impact. Generally, the positive effect of improved bottom hole cleaning is proven for all types of bits and even for rock types with low permeability, like Neuhauser

granite, dynamic hold down forces could highly affect the rate of penetration as shown by 13. Kolle et al.²⁶ assigned significant ROP enhancement to high pressure jet bottom hole cleaning. According to 24, even the simple extension of the nozzles, without any pressure-increase or changes in the flow rate, enhanced the ROP. If the created kerfs were quite shallow and the indentation depth was small due to low weight on bit, the interaction of the kerf and the inserts might have been limited. As the two-nozzle bit affected a wider area, the high pressure cleaning effect was more distinct for that type of bit. With increasing WOB, the penetration depth of the inserts increased as well and the interaction with the jetted kerf got more efficient. While the bottom hole cleaning was still contributing to the ROP increase, the beneficial impact of the jetted kerfs was more pronounced at higher weight on bit. In that regard the ROP increase could be associated with the combination of two beneficial effects, whereas bottom hole cleaning was more important at low weight on bit and kerfing at increased weight on bit. This correlation explains the observations in Fig. 8 quite well. In simplified terms it means that the two-nozzle bit is a “bottom hole cleaning bit” and the one-nozzle bit is a “kerfing bit”, whereby both effects acting simultaneously to different extent.

Another method of evaluation indicated that the beneficial impact of jet cuts was related to the mechanical rock destruction process. The rock samples were saturated with a liquid fluorescing two-component epoxy resin, as shown in Fig. 9. Following the procedure suggested by 34 ensured that all micro-cracks were filled with the epoxy resin. Partial testing of the 2–3 mm thick rock plates with a dye penetration procedure after saturation verified that no cracks were left unfilled. Micro-cracks are a direct measure of rock damage. From Fig. 11, the induced damage is clearly visible, marked with the dotted lines. Both pictures were taken from the same rock sample and the same drilling experiment. It appears that the micro-cracks were not directly created by the jet cut, but by the mechanical loading of the inserts. In the upper picture, the rock was damaged but not removed while in the lower picture the damaged area was removed. This favourable situation would obviously not have been the case without the jetted kerf. Rock damage by the inserts was amplified by the existence of the kerf that clearly contributed vitally in increasing the ROP. However, this type of rock damage was not observed to the same extent for all rock plates

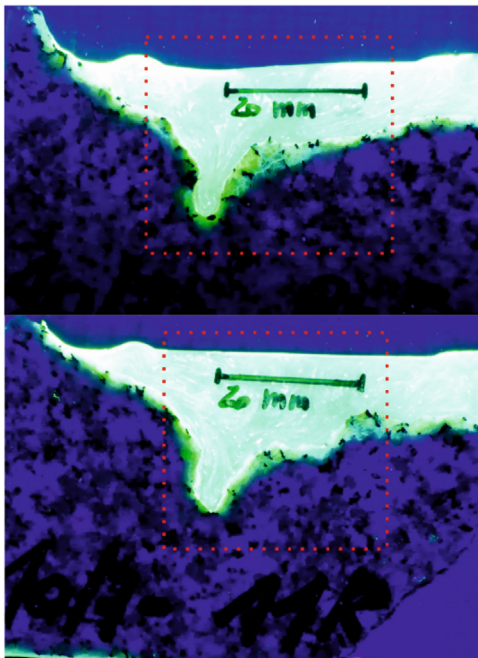


Fig. 11. Crack evaluation of bottom hole rock sample with fluorescing epoxy resin.

investigated, some samples did not show any additional damage at all. Because the mechanism behind crack generation, crack propagation and the related effects were not entirely identified yet and further effort is needed to acquire more detailed and reliable results, the presented conclusions are not complete and serve only to support the current considerations.

Regarding the identification of the relevant mechanisms for jet cutting under submerged pressurized conditions, Cheung and Hurlburt³⁵ provide a theory to predict the extent of the cavitation shroud x_c , which was modified by 3 as follows:

$$x_c = \frac{d_0}{4} \sqrt{\frac{P_j}{P_a}} \ln(0.113P_j/P_a) \quad (3)$$

where P_j is the differential pressure, P_a is the ambient pressure and d_0 is the nozzle diameter. By applying an ambient pressure of 10 MPa and as a consequence thereof a differential pressure of 210 MPa and 105 MPa, the cavitation shroud is predicted to collapse within one nozzle diameter. This conclusion was compared to another possible method to identify the contribution of cavitation on the jet cutting process. Following the mathematical and theoretical framework provided by 36, cavitation can in the first place only occur if the negative pressure coefficient C_p is greater than the cavitation number σ , calculable with the following equations:

$$-C_p = \frac{P_{ref} - P_j}{\frac{1}{2}\rho v_{ref}^2} \quad (4)$$

$$\sigma = \frac{P_{ref} - P_v}{\frac{1}{2}\rho v_{ref}^2} \quad (5)$$

The required input parameters for the calculation are actually very similar to the one required for the formula given by 3, where P_{ref} is the ambient pressure, P_j is the jet pressure, P_v is the vapour pressure, equal to 2300 Pa, and ρ is the fluid density, assumed with 1000 kg/m³. The jet exit velocity, labelled v_{ref} is estimated for incompressible flow of water via the rearrangement of Bernoulli's equation, resulting in:

$$v_{ref} = \sqrt{\frac{2P_j}{\rho}} \quad (6)$$

For a jet pressure of 220 MPa, the exit velocity calculation yields 663 m/s and 480 m/s for 115 MPa jet pressure. Applying a reference pressure of 10 MPa results in a pressure coefficient C_p of 0.955 and a cavitation number σ of 0.045 for the 220 MPa jet and a pressure coefficient C_p of 0.911 and a cavitation number σ of 0.087 for the 115 MPa jet. Hence, theoretically cavitation should have occurred at the considered conditions. Recalling the results of the calculation according to 3, the formation of cavitation bubbles around the jet was possible, but the shroud was predicted to collapse within one nozzle diameter. According to the pressure measurements, except of very short-term events, the mud pressure during the experiments was always greater than 10 MPa, therefore cavitation should not have played a role in the high pressure jet cutting performance. Thus, the dynamic pressure of the jet appears to have been the main mechanism for the rock destruction under these boundary conditions.

3.2. Comparison of drilling performance with different fluids

Interestingly, the drilling performance with mud and water was similar. Only the one-nozzle bit was tested with mud and concerning the experiments with the xanthan gum fluid, no high-pressure jet-assisted experiments were conducted at all due to technical issues with the test bench. The evaluation method was equal to the one already described in Section 3.1. The particular data points were averaged for the same conditions and are displayed as discrete points in Fig. 12. Again, the coefficient of determination was not affected by that procedure and was at the minimum 0.99, which confirms the linear relationship for all

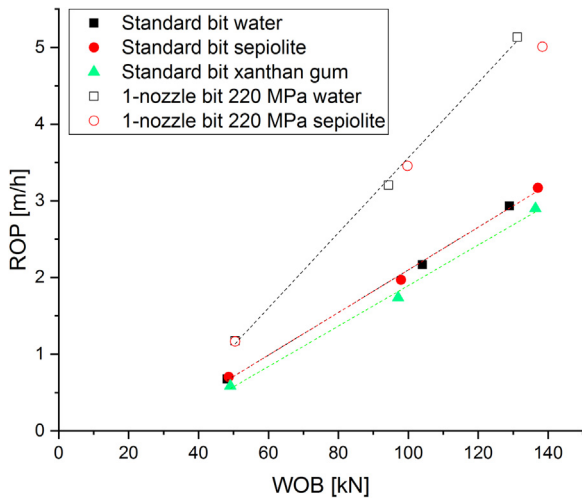


Fig. 12. Drilling performance comparison between water and mud as drilling fluid.

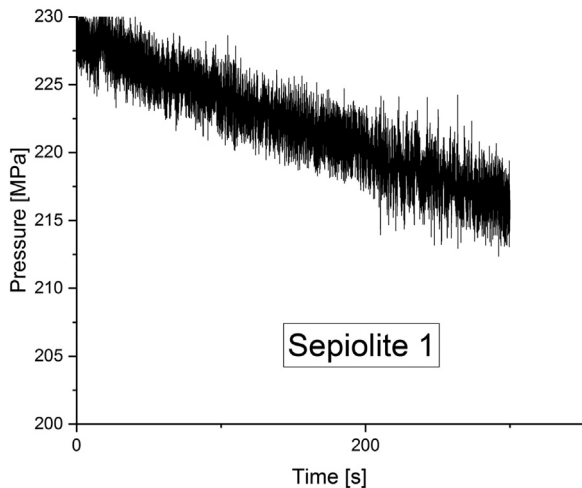


Fig. 13. Measurement from pressure transducer with sepiolite based mud.

curves. For the one-nozzle bit tests with a jet pressure of 220 MPa, the rate of penetration was equal for water and sepiolite mud at 49 kN and 98 kN WOB. The deviation at higher WOB was not related to any drilling aspect but to the reduction of the jet cutting performance. The output of the pressure transducer for one of the experiments with the

sepiolite mud is illustrated in Fig. 13 exemplarily.

Obviously, the pressure was constantly decreasing, indicating distinct nozzle erosion. While the pressure readings during experiments with water showed a constant mean value of the jet pressure, the enlarging nozzle diameter during the sepiolite tests caused the jet pressure to decrease. After the experiments, the nozzles were removed and the erosion of the nozzle was clearly visible. So, one major future activity is the research on more durable equipment. Without the pressure drop, the drilling performance for the one-nozzle bit with water and sepiolite mud would most likely have been equal, as it was for the standard bit. In order to not introduce misleading conclusions, only the coefficients A and B of the regressions analysis of the standard bit with drilling fluids were added to Table 5.

Surprisingly, the rate of penetration for the experiments with the standard bit and xanthan gum based mud was significantly lower than the ROP for experiments performed with water and sepiolite based mud, although the rheological properties of sepiolite based mud and xanthan gum based mud were adjusted to similar numbers (Yield Point) at standard API rheology test. Since the results with water and sepiolite correlate perfectly, there must be a difference between the impact of the fluid on the drilling process. Unfortunately, no data is available for jet-assisted experiments, which would have been an important addition and could maybe have led to an explanation. One possible explanation would be wear on the tungsten carbide inserts, but this was excluded after the dull analysis of the bit. Another effect could be related to the hole cleaning efficiency and a maybe increased influence of dynamic hold down for the xanthan gum based mud.

3.3. Evaluation in relation to torque on bit

The torque on bit (TOB) is usually not a very crucial parameter for drilling with roller cone bits. The torque was directly related to the weight on bit with a coefficient of determination of 0.89 for all experiments performed, shown in Fig. 14. As a consequence of that correlation, the ROP also depended quite linearly on the torque, illustrated in Fig. 14a. Furthermore, the torque constitutes the mechanical power consumption of the bit, used for rock destruction and frictional losses. A change in torque under steady-state drilling conditions would indicate a change of the drill bit properties, most likely failure of parts or the whole bit. Since no such behaviour was observed during the experiments or the later bit dull analysis, the torque measurements were generally classified as unremarkable. Though, a significant, but not excessive, higher WOB was observed for the novel drill bits compared to the baseline bit. This effect was simply the result of the increased depth per revolution. Except for one test with the one-nozzle bit at 220 MPa jetting pressure per fluid (water and sepiolite), all experiments were

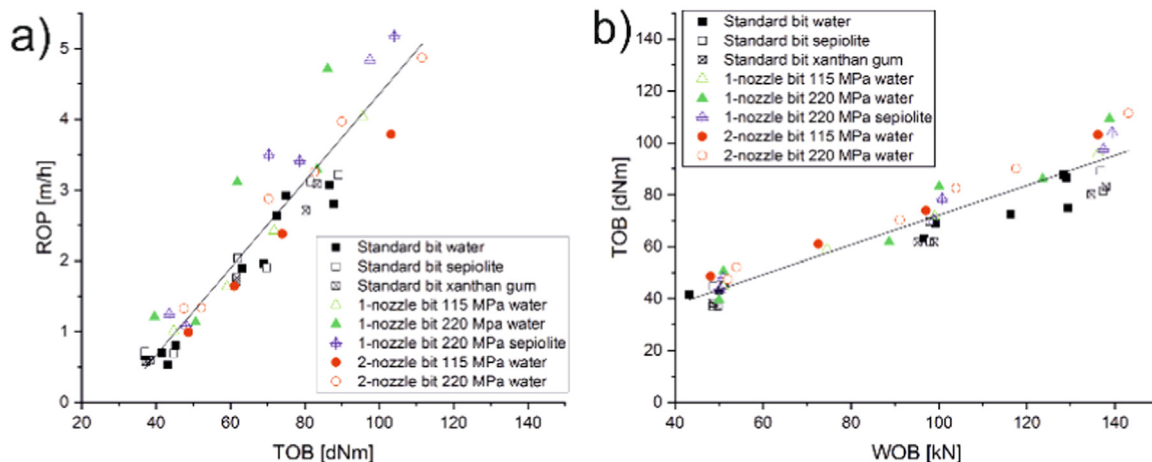


Fig. 14. (a) TOB versus ROP and (b) TOB versus WOB for all experiments.

following the same linear relationship with similar slopes. As the deviating tests did not show any signs of irregularities in terms of WOB vs. ROP or other abnormalities, no further investigations were made in that direction.

3.4. Specific energy of drilling

The important concept of specific energy in rock drilling was first introduced by 37 and 38 and the specific energy is accordingly defined as the energy required to excavate a unit volume of rock. In ordinary drilling operations the energy consumption and the specific energy for excavating the rock are determined by a thrust component E_t and a rotary component E_r , where normally E_r is far greater than E_t . The specific energy is a measure to quantify and compare the efficiency of different methods, while the total power consumption can be used to define the economical and ecological impact of the drilling process. By using the formulas provided by 38, the thrust and rotational component of the specific energy were calculated as well as the associated mechanical power P_t and P_r . Additionally, the hydraulic power P_h and specific energy E_h of the high pressure jets were calculated, utilizing the jet pressure P_j and the related flow rate Q_j . All input parameters and results are summarized in Table 6 and relevant results are illustrated in Fig. 15, where the values provided for WOB, TOB, RPM and ROP were the averaged values derived from the experiments and the residual values were calculated with the subsequent formulas. The drilled area A_d was computed as circle with the diameter of the drill bit, which was 8½ inch. Since the mud stream through the low-pressure nozzles was not directly contributing to the rock destruction process, this component was not considered in the calculations.

$$E_t = \frac{WOB}{A_d} \tag{7}$$

$$E_r = \frac{TOB \times RPM}{ROP} \tag{8}$$

$$P_t = WOB \times ROP \tag{9}$$

$$P_r = 2\pi \times RPM \times TOB \tag{10}$$

Table 6
Relevant parameters and results of the specific energy calculation.

Bit type	one-nozzle bit				two-nozzle bit											
Drilling Fluid	Water															
RPM, rev/min	60															
Drilled Area, mm ²	38,013															
Pressure of jet, MPa	115				220				115				220			
WOB, kN	50.96	98.98	136.22	50.45	94.37	131.21	48.02	97.02	136.22	52.92	97.51	130.34				
TOB, kN	447.30	717.85	956.00	450.85	740.00	977.50	486.50	739.50	1031.40	498.20	764.45	1007.40				
ROP, mm/s	0.28	0.67	1.12	0.33	0.89	1.43	0.28	0.67	1.12	0.37	0.85	1.23				
Specific energy thrust, MJ/m ³	1.34	2.60	3.58	1.33	2.48	3.45	1.26	2.55	3.58	1.39	2.57	3.43				
Specific energy torque, MJ/m ³	263.55	176.07	140.82	228.61	137.45	113.28	286.65	181.38	151.92	222.06	148.24	135.62				
Specific energy high pressure jet, MJ/m ³	9152.48	3810.01	2288.06	16,011.27	5865.22	3659.41	9846.42	4098.89	2461.54	13,488.37	5868.33	4073.98				
Hydraulic jet power, kW	97.60	97.60	97.60	198.40	198.40	198.40	105.00	105.00	105.00	190.14	190.14	190.14				
Mechanical power, kW	2.82	4.58	6.16	2.85	4.73	6.33	3.07	4.71	6.63	3.15	4.89	6.49				

Bit type	one-nozzle bit			Standard								
Drilling Fluid	Sepiolite			Water								
RPM, rev/min	60											
Drilled Area, mm ²	38,013											
Pressure of jet, MPa	220			Not high pressure jet assisted								
WOB, kN	50.46	99.76	138.38	48.22	104.01	128.90	48.63	97.90	137.09	49.10	97.07	136.37
TOB, kN	458.20	744.80	1008.05	417.45	681.79	831.43	408.64	658.98	853.43	377.65	616.80	817.30
ROP, mm/s	0.32	0.96	1.39	0.19	0.60	0.82	0.20	0.55	0.87	0.16	0.48	0.81
Specific energy thrust, MJ/m ³	1.33	2.62	3.64	1.27	2.74	3.39	1.28	2.58	3.61	1.29	2.55	3.59
Specific energy torque, MJ/m ³	233.53	128.24	119.74	367.80	187.30	168.56	345.62	198.94	162.53	382.76	211.11	167.73
Specific energy high pressure jet, MJ/m ³	16,093.56	5436.70	3750.72	-	-	-	-	-	-	-	-	-
Hydraulic jet power, kW	198.40	198.40	198.40	-	-	-	-	-	-	-	-	-
Mechanical power, kW	2.90	4.78	6.53	2.62	4.28	5.22	2.57	4.14	5.36	2.37	3.88	5.14

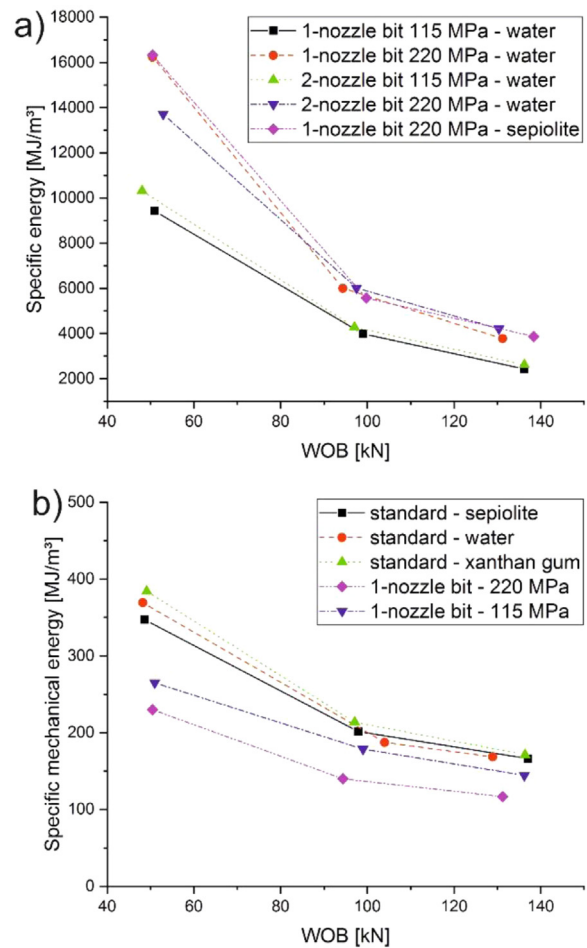


Fig. 15. (a) WOB vs specific total energy for the high pressure jet assisted bits and (b) WOB vs specific mechanical energy for the standard bit with different fluids and the one-nozzle bit with water.

$$E_h = \frac{P_h}{A_d \times ROP} \quad (11)$$

$$P_h = P_j \times Q_j \quad (12)$$

Obviously, the mechanical component of the applied specific energy as well as the total mechanical power were negligible compared to the hydraulic components. Fig. 15b emphasizes that the jetting process decreased the amount of mechanical specific energy, which demonstrates the beneficial effect of the jetted kerfs on the mechanical rock destruction process. Indeed, concerning the total components this reduction was absolutely irrelevant during the experiments. Furthermore, the efficiency in terms of total specific energy was rather similar for the one-nozzle bit and the two-nozzle bit with equal high pressure jet specifications, and also the usage of sepiolite instead of water as drilling fluid had no significant effect. As already predicted by 38 the specific energy was decreasing with increasing WOB due to reduced friction losses and increased particle size. Whereas these effects are normally only valid for common drilling operations without high-pressure fluid jets, an increased WOB caused a distinct reduction of the total specific energy, which was characterized by the hydraulic specific energy. In contrast to the thrust and rotational component the hydraulic specific energy was not changed by an increase in WOB since the supplied hydraulic power by the external pump remained the same through the whole test run. However, with increasing WOB the ROP increased as well and the jetted kerfs enabled the inserts to remove a distinctly larger volume compared to drilling without these kerfs. As a result, larger sized particles were created and reduced friction losses occurred in the sphere of the kerfs. Hence, the efficiency of the entire rock destruction process was increased with increasing WOB.

The current results yield that the hydraulic energy input into the rock during drilling was enormous. Regarding the achieved ROP - increase of around 75%, it appears that jet assisted drilling is a very inefficient method. However, some more factors have to be considered for a comprehensive assessment. Depending on the boundary conditions, such as size of the drill rig, drilling depth, inclination of the wellbore etc. torque values of several ten thousand Nm are normally applied on the drill string in the field. The hydraulic power provided by the mud pumps is usually in the order of 500–1000 kW. Losses down the drill string cause only a fraction of the surface values to be applied to the drill bit. Nevertheless, concepts are available or currently under development to use the hydraulic power of the mud stream to drive a downhole pressure generation tool. Ideally, no additional power has to be provided from surface to generate the high-pressure jets and the entire concept would indeed be very efficient. Certainly, important tasks such as cooling the bit and removing the cuttings from the borehole bottom still have to be performed properly, resulting eventually in the need for additional hydraulic power from surface. Field tests will be the most suitable method to answer that question.

4. Conclusions

Full-scale drilling experiments (8½ in. bit size) with a high-pressure fluid jet-assisted rotary drilling system were performed in hard to drill crystalline rock. The system included novel drill bits and high-pressure components. An existing drilling simulator test bench was adapted to the requirements of the current tests. In total, seventeen tests were conducted, which enabled a comparison in drilling performance between state of the art drilling techniques and the innovative jet-assisted system. Further, three different fluids were used as drilling mud and as jetting medium during the experiments. A detailed investigation on the interaction of the hydraulic and mechanical rock removing processes provides insights into the rock destruction process. Basic and sophisticated correlations between drilling process variables were examined in order to define the favourable operational parameters.

A linear relationship of the ROP and the applied weight on bit was

verified with excellent coefficients of determination. The torque on bit was also found to be linearly dependent on the WOB with reasonably high quality of regression.

The significant influence of the total hydraulic power at the bit, and especially the hydraulic power related to high pressure fluid jets, on the ROP increase was ascertained. The favourable and most effective operational conditions of each novel bit type were found to lie in different ranges of WOB while the rate of penetration was increased by a factor of more than 1.7 at a maximum, compared with the standard roller cone bit for both bit types.

The dimensions of the created jet kerfs were estimated, and the influence on the mechanical rock destruction process was qualitatively evaluated. The beneficial effect of additional free surface provided by the jetted kerfs was proven while a ROP increase attributed to improved bottom hole cleaning (improved rock cutting removal) was only assumed.

It was found that the type of fluid used had no significant influence on the drilling performance of the high-pressure jet assisted drill bits, whereas a distinct increase in the erosion rate was observed with the sepiolite based fluid.

Considering the specific energy, it turned out that the total specific energy was characterized by the hydraulic component from the high-pressure jet stream and the components due to thrust and rotation were in comparison negligible. However, increasing the WOB resulted in a decreasing total specific energy, indicating a better efficiency of the entire process. This effect occurred because the jetted kerfs enabled the inserts to remove a distinctly larger volume compared to ordinary drilling, resulting in particles of larger size and reduced friction losses in the sphere of the kerfs.

Acknowledgement

We are very thankful for the knowledgeable support of the excellent team of the technical centre of URACA GmbH & Co. KG during the preparation and execution of the tests. We also want to thank the team of the drilling laboratory in Pau for their assistance during the experiments. The help of all involved “ThermoDrill” partners was highly appreciated and we want to thank them for the outstanding team work. This project has received funding from the European Union's Horizon 2020 research and innovation programme under grant agreement no. 641202.

References

1. Stoxreiter T, Martin A, Teza D, Galler R. Hard rock cutting with high pressure jets in various ambient pressure regimes. *Int J Rock Mech Min Sci.* 2018;108:179–188.
2. Reichman JM. *Research and Development of a High-pressure Waterjet Coring Device for Geothermal Exploration and Drilling.* Report for U.S. Department of Energy; 1977.
3. Kolle JJ. Jet kerfing parameters for confined rock. In: Proceedings of the Fourth U.S. Water Jet Conference. Berkeley. 26–28 August 1987:134–144.
4. Johnson A, Eslinger D, Larsen H. An abrasive jetting scale removal system. In: Proceedings of SPE/ICoTA Coiled Tubing Roundtable. Houston. 15–16 March 1998:105–110.
5. Rowley DS, Howe RJ, Deily FH. Laboratory drilling performance of the full-scale rock bit. In: Proceedings of 35th Annual Fall Meeting of SPE. Denver. 2–5 October 1960:71–81.
6. Maurer WC. The perfect-cleaning theory of rotary drilling, 37th Annual fall meeting of SPE. Los Angeles. 7–10 October 1962:270–1274.
7. Eckel JR. Effect of pressure on rock drillability. In: Proceedings of 32nd Annual Fall Meeting of SPE. Dallas. 6–9 October 1957:1–6.
8. Cunningham RA, Eenik JG. Laboratory study of effect of overburden, formation and mud column pressures on drilling rate of permeable formations. In: Proceedings of 33rd Annual Fall Meeting of SPE. Houston. 5–8 October 1958:9–17.
9. Warren TM, Smith MB. Bottomhole stress factors affecting drilling rate at depth. *J Petrol Technol.* 1985;37:1523–1533.
10. Garnier AJ, van Lingen NH. Phenomena affecting drilling rates at depth. In: Proceedings of 33rd Annual Fall Meeting of SPE. Houston. 5–8 October 1958:232–239.
11. Vidrine DJ, Benit EJ. Field verification of the effect of differential pressure on drilling rate. In: Proceedings of SPE 42nd Annual Fall Meeting. Houston. 1–4 October. 1967:676–682.
12. Black AD, Dearing HL, DiBona BG. Effects of pore pressure and mud filtration on

- drilling rates in a permeable sandstone. *J Petrol Technol.* 1985;37:1671–1681.
13. Van Lingen NH. Bottom scavenging – A major factor governing penetration rates at depth. In: Proceedings of the 36th Annual Fall Meeting of SPE. Dallas. 8–11 October 1961:187–196.
 14. Black AD, Tibbits GA, Sandstrom JL, DiBona BG. Effects of size on Three-Cone bit performance in laboratory drilled shale. *J Petrol Technol.* 1985;25:473–481.
 15. Holster JL, Kipp RJ. Effect of bit hydraulic horsepower on the drilling rate of a polycrystalline diamond compact bit. *J Petrol Technol.* 1984;36:2110–2118.
 16. Tibbits GA, Sandstrom JL, Black AD, Green SJ. Effects of bit hydraulics on full-scale laboratory drilled shale. *J Petrol Technol.* 1981;33:1180–1188.
 17. Somerton WH. A laboratory study of rock breakage by rotary drilling. In: Proceedings of Fall Meeting of the Los Angeles Basin Section. Los Angeles. 16–17 October 1958:92–97.
 18. Warren TM. Drilling model for soft-formation bits. *J Petrol Technol.* 1981;33:963–970.
 19. TerraTek. Deeptryk phase 1 and 2 – improving deep drilling performance, report, Salt Lake City, January; 2008.
 20. Geier JE, Hood M. The effect of pre-weakening a rock surface, by waterjet kerfing, on cutting tool forces. In: Proceedings of the fourth U.S. Water Jet Conference. Berkeley. 26–28 August 1987:152–163.
 21. Fenn O. The use of water jets to assist free-rolling cutters in the excavation of hard rock. *J S Afr Inst Min Metall.* 1987;87:137–147.
 22. Kolle JJ. A model of dynamic confinement during drilling in pressurized boreholes. *Int J Rock Mech Min Sci Geomech Abstr.* 1993;30:1215–1218.
 23. Peltier B, Atkinson C. Dynamic pore pressure ahead of the bit. In: Proceedings of IADC/SPE Drilling Conference. Dallas. 10–12 February 1986:351–358.
 24. Feenstra R van Leeuwen JJM. Full-scale experiments on jets in impermeable rock drilling. SPE Annual fall meeting. New Orleans. 6–9 October 1968:329–336.
 25. Wells MR. Dynamics of rock-chip removal by turbulent jetting, SPE Annual technical Conference and exhibition, Las Vegas. 22–25 September 1985:144–152.
 26. Kolle JJ, Otta R, Stang DL. Laboratory and field testing of an ultra-high-pressure, jet assisted drilling system. In: Proceedings of SPE/IADC Drilling Conference. Amsterdam. 11–14 March; p. 847–857.
 27. Veenhuizen SD, Kolle JJ, Rice CC, O'Hanlon TA. Ultra-high pressure jet assist mechanical drilling, SPE/IADC Drilling conference. Amsterdam. 4–6 March 1997:79–90.
 28. Veenhuizen SD, Stang DL, Kelley DP, Duda JR, Aslakson JK. Development and Testing of Downhole Pump for High-Pressure Jet-Assist Drilling. SPE Annual Technical Conference and Exhibition. San Antonio. 5–8 October 1997.
 29. Butler T, Fontana P, Otta R. A method for combined jet and mechanical drilling. In: Proceedings of the 65th Annual Technical Conference and Exhibition of SPE. New Orleans. 23–26 September 1990:561–565.
 30. Liao H, Guan Z, Shi Y, Liu Y. Field tests and applicability of downhole pressurized jet assisted drilling techniques. *Int J Rock Mech Min Sci.* 2015;75:140–146.
 31. Robinson LH, Ramsey MS. Onsite Continuous Hydraulics Optimization (OCHO). In: Proceedings of AADE National Drilling Technical Conference. Houston. 27–29 March 2001.
 32. Diethart-Jauk E, Gegenhuber N. Shear weakening for different lithologies observed at different saturation stages. *J Appl Geophys.* 2018;148:107–114.
 33. Gnirk PF, Cheatham JB. A theoretical description of rotary drilling for idealized down-hole bit/rock conditions. In: Proceedings of 43rd Fall Annual SPE meeting. Houston. 29 September–2 October 1968:443–450.
 34. Entacher M, Schuller E, Galler R. Rock failure and crack propagation beneath disc cutters. *Rock Mech Rock Eng.* 2015;48:1559–1572.
 35. Cheung JB, Hurlburt GH. Submerged water-jet cutting of concrete and granite. In: Proceedings of the Third International Symposium on Jet Cutting Technology. Chicago. 11–13 May 1979:E5–E49.
 36. Wright MM, Epps B, Dropkin A, Truscott TT. Cavitation of a submerged jet. *Exp Fluids.* 2013;54:1541.
 37. Simon R. Energy Balance in Rock Drilling. SPE-U. In: Proceedings of Texas Drilling and Rock Mechanics Symposium. Austin. 23–24 January 1963:298–306.
 38. Teale R. The concept of specific energy in rock drilling. *Int J Rock Mech Min Sci.* 1965;2:57–73.